Structure of Random Foam

Andrew M. Kraynik,[1,*] Douglas A. Reinelt,[2] and Frank van Swol[3]

[1]*Sandia National Laboratories, Department 9114 MS0834, Albuquerque, NM 87185-0834, USA*
[2]*Department of Mathematics, Southern Methodist University, Dallas, TX 75275-0156, USA*
[3]*Sandia National Laboratories, Department 1834 MS1411, Albuquerque, NM 87185-1411, USA*

(Received 22 June 2004; published 9 November 2004)

The Surface Evolver was used to compute the equilibrium microstructure of dry soap foams with random structure and a wide range of cell-size distributions. Topological and geometric properties of foams and individual cells were evaluated. The theory for isotropic Plateau polyhedra describes the dependence of cell geometric properties on their volume and number of faces. The surface area of all cells is about 10% greater than a sphere of equal volume; this leads to a simple but accurate theory for the surface free energy density of foam. A novel parameter based on the surface-volume mean bubble radius R_{32} is used to characterize foam polydispersity. The foam energy, total cell edge length, and average number of faces per cell all decrease with increasing polydispersity. Pentagonal faces are the most common in monodisperse foam but quadrilaterals take over in highly polydisperse structures.

DOI: 10.1103/PhysRevLett.93.208301 PACS numbers: 82.70.Rr

Foam conjures up images of cellular patterns that are disordered and polydisperse as in soap froth—the quintessential foam and subject of this Letter. Random cellular morphology is the hallmark of low-density liquid and solid foams, and describes self-assembled systems such as liquid-liquid emulsions, block copolymers, and micelles. Moreover, phase boundaries in polycrystals, Voronoi partitions of amorphous materials (simple liquids, glass, and granular solids), and the clustering of galaxies are also foam-like [1–3].

Scientists and mathematicians have been contemplating the structure of soap froth for over a century, often focusing on idealized systems that are ordered and monodisperse in response to the Kelvin problem [4]: partitioning three-dimensional space into equal-volume cells and minimum surface area. Ordered foams are not very diverse; collectively they only contain a few kinds of cells [5–8]. Real foams, by contrast, are disordered and contain an impressive variety of cell shapes, even when the bubbles have equal volumes; e.g., Matzke [9] found 36 types of polyhedra among 600 foam cells and many more occurred in our recent Surface Evolver [10,11] simulations of random monodisperse foams [12]. The simulations largely confirm the topological statistics reported by Matzke and provide accurate geometric properties of foams and individual cells. We are now simulating random foams with a wide range of cell-volume distributions. This is a key step toward understanding the physics of real materials that evolve through diffusive coarsening [13–15] and exhibit rich rheological behavior [2,16]. The cells in these jammed systems [17] experience geometrical frustration and are subject to long-range correlations. The environment is fundamentally different from single cells surrounded by neighbors that have equal pressures [18] or finite bubble clusters [19]. Experimental studies of bidisperse [20] and slightly polydisperse [21] foams typically involve $O(10^2)$ bubbles and many of them contact container walls. We have simulated large spatially periodic structures that contain 1728 cells and represent bulk foams. The models provide statistically significant results that reveal universal topological and geometric properties of random foams and the cells in them. For example, we find that geometric properties (surface area, edge length, mean curvature) of the bubbles are described extremely well by an analytical theory [22] for idealized foam cells called *isotropic Plateau polyhedra* (IPP), which have F identical, spherical-cap faces and satisfy Plateau's laws. This is remarkable because the faces on a typical cell have different shapes (number of edges, etc.) and are not spherical caps; and furthermore, the only constructible IPP are those with the symmetry of Platonic solids: the tetrahedron, cube, and dodecahedron. The success of the theory indicates that the primary dependence of metric properties on cell shape is captured by F, the number of faces.

We consider the dry foam limit where liquid volume fraction is negligible. Thin films stabilized by surfactants are represented as two-dimensional surfaces constrained by Plateau's rules for mechanical equilibrium and area minimization. The cells are trivalent polyhedra; the faces are surfaces of constant mean curvature that meet at dihedral angles of 120°; and the cell edges meet at the tetrahedral angle $\arccos(-1/3) \approx 109.47°$.

The basic strategy used to model random monodisperse foams [12] was modified to produce polydisperse foams. First, molecular dynamics is used to generate dense packings of hard, polydisperse spheres; the final densities range from 0.64 (identical spheres) to 0.72 for highly nonuniform systems. Then, Laguerre (weighted-Voronoi) tessellations are used to fill space with convex polyhedral cells that enclose the different-size spheres and set the cell-volume distribution. Foam polydispersity is controlled by selecting a probability distribution for sphere diameters (log-normal, gamma, or Gaussian), a

standard deviation, and, if necessary, a maximum diameter to prevent the formation of extremely large cells. The Surface Evolver [10,11] is then used to relax the Laguerre structures to satisfy Plateau's laws (see [12] for details). Convergence to a local energy minimum involves hundreds of topological transitions that are triggered by cell edges shrinking to zero length. Subjecting the foam to large-deformation, tension-compression cycles, a process we call annealing, provokes more topological transitions and drives the foam into a deeper energy minimum. Monodisperse foams can be relaxed by using n flat (linear) triangular facets to approximate the shape of each face (n-gon) because the curvatures are relatively small. Polydisperse foams, however, require the use of curved (quadratic) facets to fully relax the foam because the surface curvatures are large. Finally, a slight distortion of the cubic unit cell is required to achieve isotropic stress. Simulating foam structures with 1728 cells takes anywhere from a few days to a month on a 1.2 GHz processor, depending on the amount of annealing.

Results that will be discussed below inspire a new measure of foam polydispersity that is based on the surface-volume (Sauter) mean bubble radius $R_{32} = \langle R^3\rangle/\langle R^2\rangle$, where R is the equivalent sphere radius determined from $V = \frac{4}{3}\pi R^3$, V is cell volume, and $\langle\cdot\rangle$ is number average. The polydispersity parameter p is defined by

$$p = R_{32}/\langle R^3\rangle^{1/3} - 1 = \langle R^3\rangle^{2/3}/\langle R^2\rangle - 1. \qquad (1)$$

Note that p is non-negative and equal to zero only when the foam is monodisperse.

The foam shown in Fig. 1 contains cells that vary by 2 orders of magnitude in volume, which indicates that $p \approx 0.1$ corresponds to significant polydispersity. In the most polydisperse structures that we produced, V varies by $O(10^3)$ and p reaches 0.47. The smallest cells are tetrahedra, triangular prisms, cubes, etc. [23]; the largest cells have up to 170 faces; and the faces have three to 12 edges. The cell inventory includes thousands of unique shapes, which are all trivalent polyhedra.

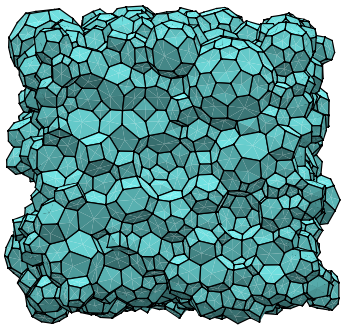

FIG. 1 (color online). Random foam with 1000 cells and polydispersity $p = 0.108$. The cell volumes vary by 2 orders of magnitude.

We now present some topological and geometric properties of simulated foams. The probability distribution functions, $\rho(F)$, that a cell has F faces and, $\rho(n)$, that a face has n edges, are shown in Fig. 2 for representative p. The distributions are narrowest for monodisperse foams where $\langle F\rangle = 13.7$; most cells have 12 to 16 faces; and most faces have four to six edges [9,12]. The small cells in polydisperse foam have fewer faces and the large cells have more faces than monodisperse foam; consequently, $\rho(F)$ is broader for polydisperse foams. The first two moments of $\rho(F)$, the mean, $\mu_1 = \langle F\rangle$, and the normalized variance, $\mu_2/\langle F\rangle^2 = \langle F^2\rangle/\langle F\rangle^2 - 1$, are plotted against p in Fig. 3. The average cell always has six sides in "Flatland" but $\langle F\rangle$ is not constant in three dimensions: $\langle F\rangle$ decreases as p increases and the peak shifts from 14 to seven neighbors. The lowest $\langle F\rangle$ that we achieved was 11.3; the theoretical lower limit of eight can be approached by successively decorating foam vertices with tetrahedral cells [24], in which case triangular faces are most abundant. The variance μ_2, the standard measure of topological disorder in foam, increases with volumetric disorder, i.e., polydispersity. Compared to $\rho(F)$, the face distribution $\rho(n)$ is less sensitive to polydispersity, especially when p is small. The height of the sharp peak at pentagonal faces decreases as p increases and is eventually surpassed by quadrilateral faces when p is large. We are not aware of any direct observations of foam structure where a maximum below pentagonal faces has been reported. Figure 3 also shows a more conventional measure of polydispersity, $\sigma_R/\langle R\rangle$, where σ_R is the standard deviation of R. The empirical relation, $\sigma_R/\langle R\rangle = 0.95p^{1/2}$, fits the data quite well.

Perhaps our most significant and surprising discovery involves the surface area S of individual foam cells. The

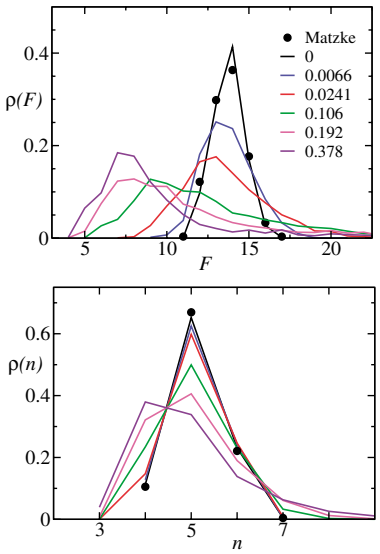

FIG. 2 (color online). Distribution of cells with F faces and faces with n edges in foams with different polydispersity p compared with Matzke's data for random monodisperse foam.

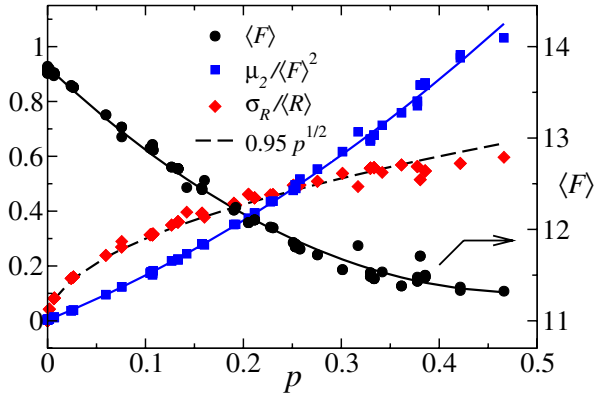

FIG. 3 (color online). Average face count $\langle F\rangle$, topological disorder $\mu_2/\langle F\rangle^2$, and an alternate measure of polydispersity $\sigma_R/\langle R\rangle$, graphed against p. The solid lines are quadratic fits to guide the eye and the dashed line is $0.95p^{1/2}$.

reduced surface-to-volume ratio β is defined as S scaled by the area of an equal-volume sphere:

$$\beta = S/(36\pi V^2)^{1/3}. \tag{2}$$

Figure 4 shows β vs F for a typical foam; β is very insensitive to F as predicted by IPP theory [22]. Simulations for many foams reveal that β has a very narrow range: 1.100 ± 0.008. Higher values of β (1.13 ± 0.02) have been calculated by numerically reconstructing optical tomography data for slightly polydisperse foam [21].

Figure 4 also includes Laguerre polyhedra from the initial condition for the foam. These flat-faced cells show strong F dependence, in accord with theory for convex isotropic polyhedra (CIP) [22], and large dispersion. The CIP theory appears to be a lower bound on β for Laguerre polyhedra; however, IPP theory is not a lower bound for foam cells because they can approach spherical shape when the surface area of $F-1$ faces goes to zero. Most foam cells lie above IPP theory; the rare exceptions have relatively few faces (five to eight) and typically one face is much larger than the others.

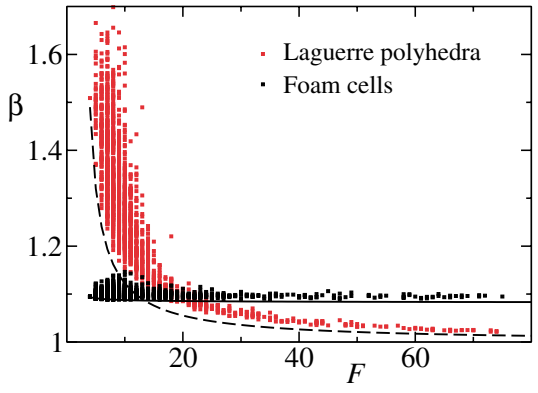

FIG. 4 (color online). Reduced surface-to-volume ratio β of foam cells and Laguerre polyhedra compared with theory for isotropic Plateau polyhedra (IPP, solid line) and convex isotropic polyhedra (CIP, dashed line).

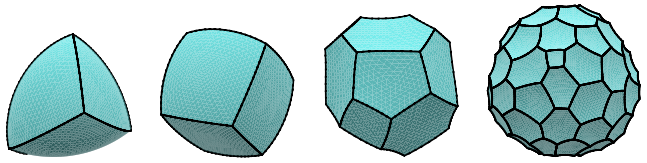

FIG. 5 (color online). Typical foam cells with four, six, 14, and 60 faces.

Foam relaxation reduces the surface area of small cells, which have fewer faces, and increases the area of large cells that have many faces. The cells shown in Fig. 5 illustrate why this occurs. The faces on cells with small F curve outward; β is smaller than when the faces are flat. The faces on cells with large F curve inward; the surface area is increased by the "dimples," as in a golf ball.

By assuming that β is constant we can derive a very simple theory for the surface free energy density of foam, defined as

$$E = \sigma S_f = \sigma \frac{\sum S}{\sum V}, \tag{3}$$

where σ is surface tension and S_f is total surface area per unit volume of foam. Using Eqs. (1) and (2) leads to

$$E = 3\beta \frac{\sigma}{R_{32}} = \frac{(36\pi)^{1/3}\beta}{1+p} \frac{\sigma}{\langle V\rangle^{1/3}}. \tag{4}$$

The length scale R_{32} captures the effect of cell size and polydispersity in a single parameter. By choosing a different characteristic length $\langle V\rangle^{1/3}$ based on average cell volume, the influence of cell size and polydispersity are separated. Excellent agreement between the theory with $\beta = 1.10$ and simulations is evident in Fig. 6.

Simulations of random soap froth provide a foundation for understanding the cellular morphology of all liquid and solid foams. Dry soap froth can be viewed as the skeleton for real foams, which have finite amounts of continuous phase, and used to estimate surface area, edge

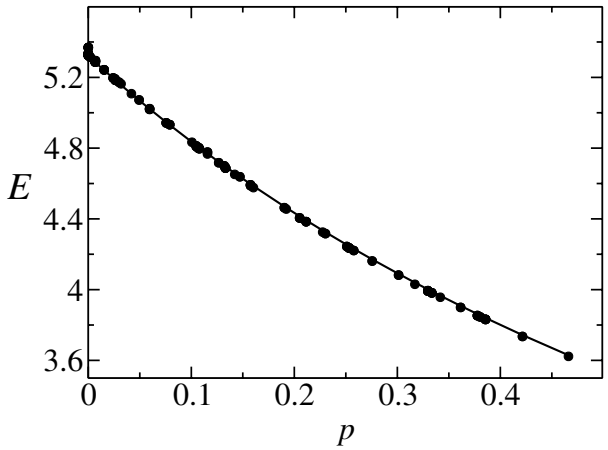

FIG. 6. Foam energy E (or specific surface area $S_f\langle V\rangle^{1/3}$) plotted against polydispersity p and compared to the theory in Eq. (4) with $\beta = 1.10$. E is scaled by $\sigma/\langle V\rangle^{1/3}$.

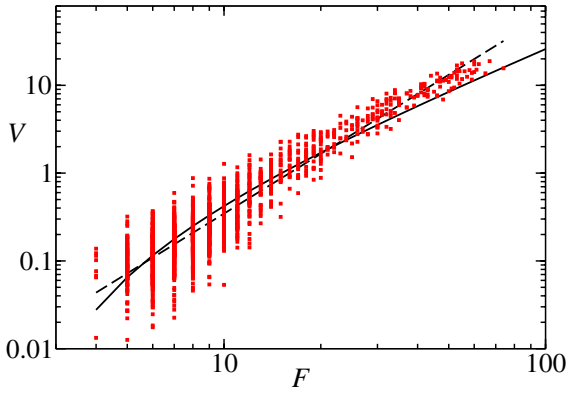

FIG. 7 (color online). V vs F for each cell in a foam with $p = 0.333$. The power-law fit with exponent $\nu = 2.262$ (dashed line) and IPP theory with $\lambda = 0.43$ (solid line) are shown for comparison.

length, and other features. For example, the liquid (solid) volume fraction ϕ of a slightly wet (low-density, open-cell) foam is given by $\phi = AL_f$, where A is the cross-sectional area of the Plateau borders (solid struts) and L_f is the total edge length per unit volume of foam. Area A is a key parameter in foam drainage [2] and the mechanics of solid foam [1]. The normalized edge length $L/V^{1/3}$ of foam cells exhibits $F^{1/2}$ behavior [18,19] as predicted by IPP theory. The corresponding macroscopic quantity L_f is slightly larger than the specific surface area S_f when both are scaled by $\langle V\rangle^{1/3}$. The empirical relation

$$L_f\langle V\rangle^{2/3} = S_f\langle V\rangle^{1/3} + 0.063 \qquad (5)$$

is accurate to within 1% when $p \lesssim 0.1$. Equations (4) and (5) relate the total edge length L_f to polydispersity p.

The two key parameters that determine cell geometric properties are volume and number of faces, and the relationship between them is complex. Figure 7 shows that the dispersion can exceed an order of magnitude, especially when F is small. Assuming power-law behavior, $V \propto F^{\nu}$, the exponent is zero for monodisperse foam and rises rapidly to $\nu = 2.268 \pm 0.056$ when $p \gtrsim 0.05$. Assuming that *all cell edges have equal length* λ, IPP theory gives a one-parameter equation for $V(F)$, which has large F behavior: $V \approx 0.3716\lambda^3(F^{3/2} - 1.6889)$. The power-law fit and IPP theory are compared in Fig. 7; both are satisfactory but neither is accurate. Potts model simulations [25] predict stronger F dependence ($V \propto F^3$) and the assumption that *all faces have equal area* predicts weaker F dependence ($V \propto F^{3/2}$) than we observe.

The results just presented cover some properties of foams and cells; other results on rheology (shear modulus and finite elasticity), cell growth rate for diffusive coarsening (von Neumann relations), and cell-neighbor correlations (Aboav-Weaire law) will be reported elsewhere. MRI and x-ray microtomography are being used to image and reconstruct liquid and solid foams [26,27]. Preliminary comparisons between simulations and measurements are very promising.

We thank Ken Brakke for implementing new algorithms to perform topological transformations in the Surface Evolver. S. Hilgenfeldt, G. Seidler, and E. Miller provided useful feedback on early drafts. Sandia is a multiprogram laboratory operated by Sandia Corporation, a Lockheed Martin Company, for the U.S. Department of Energy's National Nuclear Security Administration under Contract No. DE-AC04-94AL85000.

*Electronic address: amkrayn@sandia.gov

[1] L. J. Gibson and M. F. Ashby, *Cellular Solids: Structure and Properties* (Cambridge University Press, Cambridge, England, 1997), 2nd ed.
[2] D. Weaire and S. Hutzler, *The Physics of Foams* (Oxford University Press, Oxford, 1999).
[3] S. Perkowitz, *Universal Foam: From Cappuccino to the Cosmos* (Walker & Company, New York, 2000).
[4] *The Kelvin Problem*, edited by D. Weaire (Taylor & Francis, London, 1996).
[5] W. Thomson (Lord Kevin), Philos. Mag. **24**, 503 (1887).
[6] R. E. Williams, Science **161**, 276 (1968).
[7] D. Weaire and R. Phelan, Philos. Mag. Lett. **69**, 107 (1994).
[8] N. Rivier, Philos. Mag. Lett. **69**, 297 (1994).
[9] E. B. Matzke, Am. J. Bot. **33**, 58 (1946).
[10] K. A. Brakke, Experimental Mathematics **1**, 141 (1992).
[11] See K. Brakke, http://www.susqu.edu/facstaff/b/brakke/evolver/.
[12] A. M. Kraynik, D. A. Reinelt, and F. van Swol, Phys. Rev. E **67**, 031403 (2003).
[13] C. P. Gonatas, J. S. Leigh, A. G. Yodh, J. A. Glazier, and B. Prause, Phys. Rev. Lett. **75**, 573 (1995).
[14] C. Monnereau and M. Vignes-Adler, Phys. Rev. Lett. **80**, 5228 (1998).
[15] S. Hilgenfeldt, A. M. Kraynik, S. A. Koehler, and H. A. Stone, Phys. Rev. Lett. **86**, 2685 (2001).
[16] A. M. Kraynik, Annu. Rev. Fluid Mech. **20**, 325 (1988).
[17] *Jamming and Rheology: Constrained Dynamics on Microscopic and Macroscopic Scales*, edited by A. J. Liu and S. R. Nagel (Taylor & Francis, London, 2001).
[18] S. J. Cox and M. A. Fortes, Philos. Mag. Lett. **83**, 281 (2003).
[19] S. J. Cox and F. Graner, Phys. Rev. E **69**, 031409 (2004).
[20] E. B. Matzke and J. Nestler, Am. J. Bot. **33**, 130 (1946).
[21] C. Monnereau, B. Prunet-Foch, and M. Vignes-Adler, Phys. Rev. E **63**, 061402 (2001).
[22] S. Hilgenfeldt, A. M. Kraynik, D. A. Reinelt, and J. M. Sullivan, Europhys. Lett. **67**, 484 (2004).
[23] M. Hucher and J. Grolier, C. R. Acad. Sc. Paris **A284**, 219 (1977).
[24] M. A. Fortes, Acta Metall. **34**, 33 (1986).
[25] J. A. Glazier, Phys. Rev. Lett. **70**, 2170 (1993).
[26] G. T. Seidler, L. J. Atkins, E. A. Behne, U. Noomnarm, S. A. Koehler, R. R. Gustafson, and W. T. McKean, Adv. Complex Systems **4**, 481 (2001).
[27] M. D. Montminy, A. R. Tannenbaum, and C. W. Macosko, J. Colloid Interface Sci. **280**, 202 (2004).